



PROCESSING OF ALUMINUM ALLOY EN AW 7075 USING SELECTIVE LASER MELTING: INITIAL STUDY

Petr SKALICKÝ¹, Daniel KOUTNÝ¹, Libor PANTĚLEJEV², David PALOUŠEK¹

¹*Institute of Machine and Industrial Design, Brno University of Technology, Faculty of Mechanical Engineering, Technická 2896/2, Brno 616 69, Czech Republic*

²*Department of Material Science, Brno University of Technology, Faculty of Mechanical Engineering, Technická 2896/2, Brno 616 69, Czech Republic*

Abstract

Selective Laser Melting (SLM) is an additive manufacturing process, that uses a fine metallic powder to produce complex parts. Unfortunately, the range of SLM processed materials is limited by available materials in powder form and for many materials process parameters have not been defined. Currently, about four aluminum alloys has been successfully processed. The aim of this paper was description the influence of the process parameters to the material processability of high strength aluminum alloy EW AW 7075 by SLM. Wide range of process parameters (100-400 W laser power and 300-1400 mm/s scanning speed) were examined to find the optimum processing parameters producing homogeneous material. In this study, maximum relative density of 96.2 % was achieved. However, typical hot cracks, which appears during welding process of aluminum alloy EN AW 7075, was observed in all parts. Cracks were reduced but were not eliminated.

Key words: EN AW 7075, Selective Laser Melting (SLM), relative density, hot crack.

INTRODUCTION

Selective Laser Melting (SLM) is one of the additive manufacturing technologies, which uses fine metal powder to produce high quality parts with complex shape. SLM is most commonly used in medicine, aerospace or automotive for manufacturing of components with complicated geometry which cannot be produced by conventional methods (Olakanmi, Cochrane, & Dalgarno, 2015). Parts are manufactured directly from 3D data, layer by layer. In each layer a laser beam is used to melt the powder into solid metal only in areas corresponding to cross section of the part.

SLM fabrication process and the also quality of the final product is controlled by many process parameters, which can be sorted as laser related, scanning related, powder related and temperature related.

In many current studies on the optimization of material homogeneity e.g. (Thijs, Verhaeghe, Craeghs, Humbeeck, & Kruth, 2010) (Prashanth, Scudino, Maity, Das, & Eckert, 2017) the authors used energy density E [J/mm³], defined in equation (1), to better compare the influence of dependent parameters on the porosity and final quality of the manufactured parts. It consider the main influence parameters such as laser power P_L (W), scanning speed v_s (mm/s), hatch distance h_d (mm), layer thickness l_t (mm). These process parameters mainly affect the formation of porosity in the manufactured components (Aboulkhair, Everitt, Ashcroft, & Tuck, 2014).

$$E = \frac{P_L}{v_s \cdot h_d \cdot l_t} \quad (1)$$

The most used aluminum alloys for the production by SLM technology are Al-Si alloys. These alloys are used due to their good weldability. Aluminum alloys AlSi10Mg and AlSi12 were extensively studied, and the influence of process parameters to its behavior and mechanical properties were thoroughly described (Wei, et al., 2017), (Li, et al., 2016), (Zaretsky, Stern, & Frage, 2017), (Tang & Pistorius, 2017), (Siddique, Imran, Wycisk, Emmelmann, & Walther, 2015), (Vora, Mumtaz, Todd, & Hopkinson, 2015). These alloys in casted state have relatively poor mechanical properties compared to the 7-series (7xxx) high strength aluminum alloys. Aluminum alloy EN AW 7075 (AlZn5.5MgCu) is one of the aluminum alloys which achieves the best mechanical properties. In wrought state it has a high tensile strength of over 500 MPa and hardness of up to 160 HB. The main potential of this alloy is the high strength-weight ratio in combination with good corrosion resistance (Reschetnik, et al., 2016) (Michna



& Lukáč, 2005), however, up to now only several authors dealt with the processing of this alloy (Kaufmann, et al., 2016), (Montero Sistiaga, et al., 2016). Therefore the aim of this paper is to describe the influence of the process parameters to the material processability.

MATERIALS AND METHODS

Fabrication of samples

For this research was used SLM 280 HL (SLM Solutions, Germany) machine equipped with 400 W ytterbium fiber laser. All samples were manufactured with layer thickness 50 μm , hatch distance 0.10 mm, meander 79° as a scan strategy. Meander 79° means that each layer is scanned in both directions with a (n + 1) layer rotation of 79°. The building chamber was filled up with argon and overpressured of 10-12 mbar with maximum oxygen level of 0.2 %. The range of laser power was 100-400 W, and range of scanning speed was 50-1500 mm/s. To optimize process parameters and to achieve the highest relative density, were used cube samples of dimensions (10 x 10 x 10 mm) fitted with a truncated pyramid on the underside and were built directly on the building platform. The truncated pyramid reduces the contact area of the cube sample with the building platform and thus reduces the cooling rate. The relative density was measured in the cube part of the sample.

Powder characterization

The metal powder EN AW 7075, produced by gas atomization, was supplied by LPW Technology. Tab. 1 shows the chemical composition provided by supplier LPW Technology. Particle size distribution was measured using Horiba LA-950 particle size analyzer. Results show (Fig. 1) that powder has Gaussian distribution while particle size below 26 μm represents 10 % and particles size below 64 μm represents 90 % of the total amount of particles. Particle median size is 41.5 μm , mean size is 43.9 μm and therefore layer thickness of 50 μm was used in all experiments.

Tab. 1 Chemical composition limits of standard material and powder material

Weight %	Al	Zn	Mg	Cu	Fe	Cr	Si	Mn	Ti	Other
DIN EN 573-3	Bal	5,1-6,1	2,1-2,9	1,2-2	$\leq 0,5$	0,18-0,28	$\leq 0,4$	$\leq 0,3$	$\leq 0,2$	$\leq 0,15$
SLM powder	Bal	5,9	2,4	1,5	0,07	0,27	0,4	0,26	0,01	

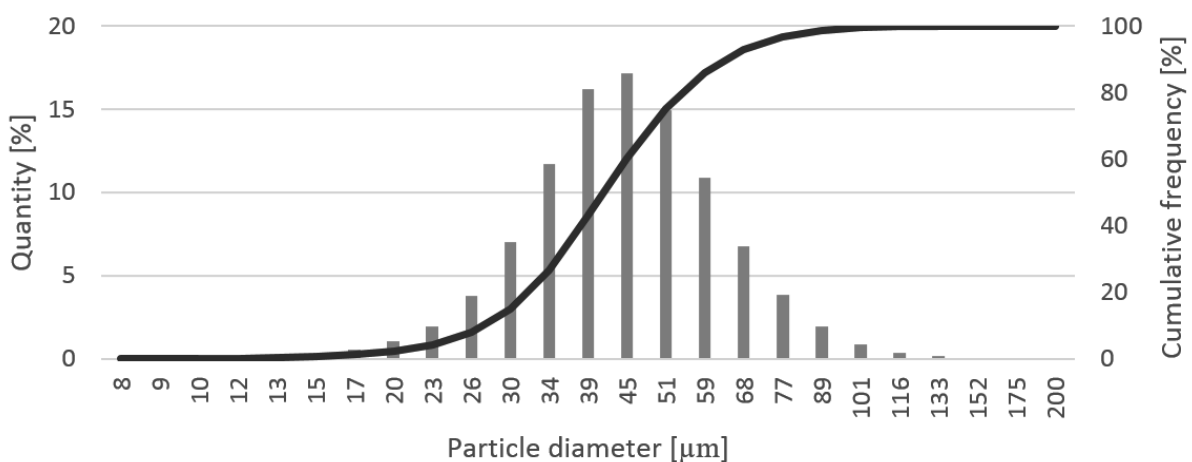


Fig. 1 Particle distribution of alloy EN AW 7075



Porosity analysis

To analyze the porosity, samples were grinded and polished, parallel to building direction, using metallographic grinder Leco GPX300 (LECO Instrumente, USA). To observe microstructure of material, samples were etched by FUSS etchant. Relative density was measured by image analysis in freeware software *Image J*, from images of samples taken on the OLYMPUS SZX7 microscope. The main investigated parameter was relative density, which includes both, pores and cracks. The selected region for the relative density analysis contained only the inner region of the sample (no contour).

RESULTS AND DISCUSSION

Cube samples were fabricated to describe the behavior of the material over a wide range of process parameter combinations and the influence of these process parameters on relative density.

The experiment was performed with hatch spacing 100 μm . Building platform was preheated to 200 $^{\circ}\text{C}$. Fig. 2 shows polished sample images sorted by the combination of used laser power and scanning speed. Each samples image contains a relative density value and energy density value. If the energy density is less than 60 J/mm^3 , the samples contain a lot of keyhole pores (see dotted area in Fig. 2). Large metallurgical pores are visible on samples manufactured with laser power 300 W and 400 W and energy density higher than 100 J/mm^3 (see dashed area in Fig. 2), but large metallurgical pores did not appear in samples with a laser output of 200 W. Cracks were visible throughout the range of process parameters. Lowering scanning speed reduces pores and cracks in samples with a laser power of 200 W, but cracks did not disappear completely. The best results of relative density 93.6 % was achieved using laser power of 300 W and a scanning speed 800 mm/s. However, results of relative density did not match with relative density values reported by (Kaufmann, et al., 2016). Fig. 3 shows, that (Kaufmann, et al., 2016) used only grinded samples in their research. This was verified on the sample with the same process parameters (laser power 400 W and scanning speed 1200 mm/s). Similar relative density was found in the grinded sample, but polishing revealed defects that were not seen after grinding. The difference in measured relative density was approximately 15 % (Fig. 3). This implies, that the cracks are most probably present in Kaufmann's study as well, however due to inappropriate technique it were not detected.

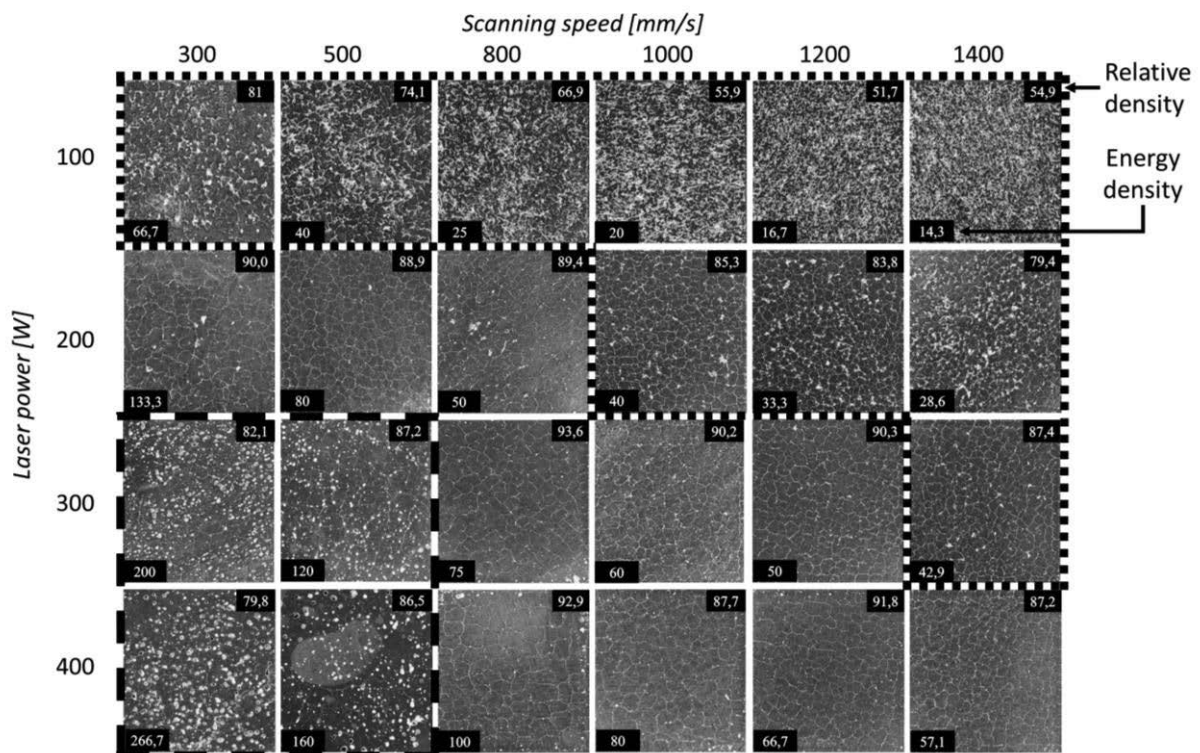


Fig. 2 Images of polished samples, relative density [%] (top right of images), energy density [J/mm^3] (bottom left of images)

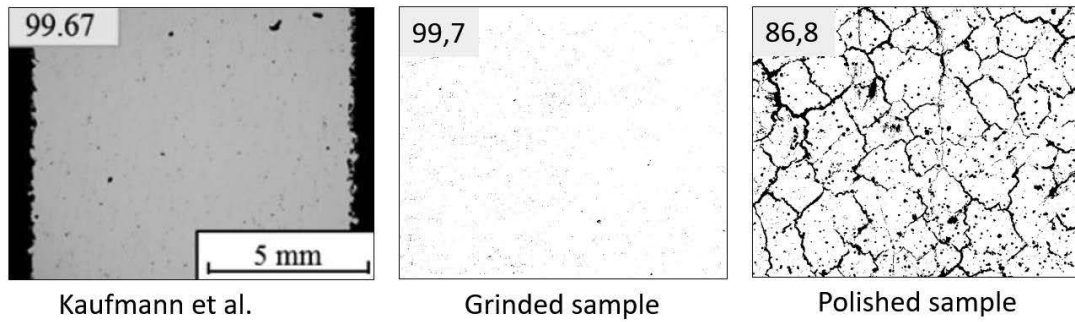


Fig. 3 Comparison of grinded sample and polished sample, relative density (top left of image)

Comparison of the relative density depending on the scanning speed for four values of laser power is shown in Fig. 4. In the case of the 300 W and 400 W laser power, the relative density increase with increasing scanning speed. If the scanning speed is higher than 800 mm/s, the relative density is stabilized around 90 %. Dependence of relative density and scanning speed for laser power 200 W shows that the relative density is not decreasing for scanning speeds below 600 mm/s as in case of 300W and 400 W L_p . Figure 4 also shows that use of 100 W laser power is inappropriate to reach higher relative density of material.

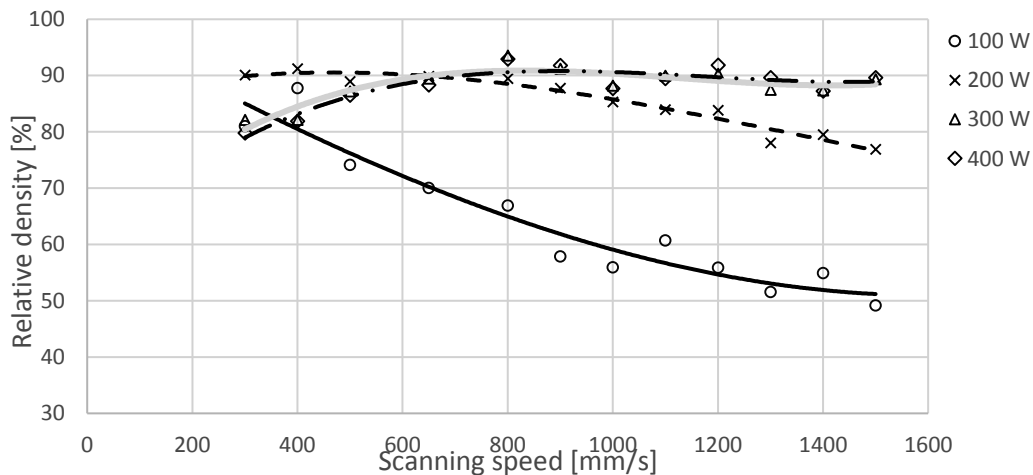


Fig. 4 Influence of scanning speed on relative density

Dependence of relative density and energy density in figure 6 show that between 50-80 J/mm³ energy density, the process for 200, 300 and 400 W laser power is stabilized with relative density about 90 %. Figures 3 and 5 shows that the cracks form a substantial part of the defective area, which is included to calculation of porosity. Thus the minimization of crack occurrence in future would improve the relative density values as well.

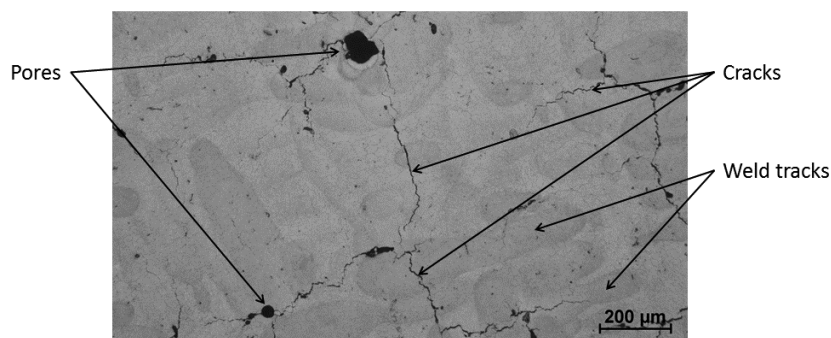


Fig. 5 Etched sample of SLM processed EN AW 7075 alloy showing microstructure with cracks



Microstructure in figure 5 show that cracks are preferentially oriented in scanning direction. During production of the next layer, cracks from both layers are interconnected and create a "net of cracks" (Fig. 3). This behavior is most probably due to high cooling rate of the SLM processing, because the semi-solid state of weld is present very short time and thus the high tension in material is induced as described by (Hu & Richardson, 2006).

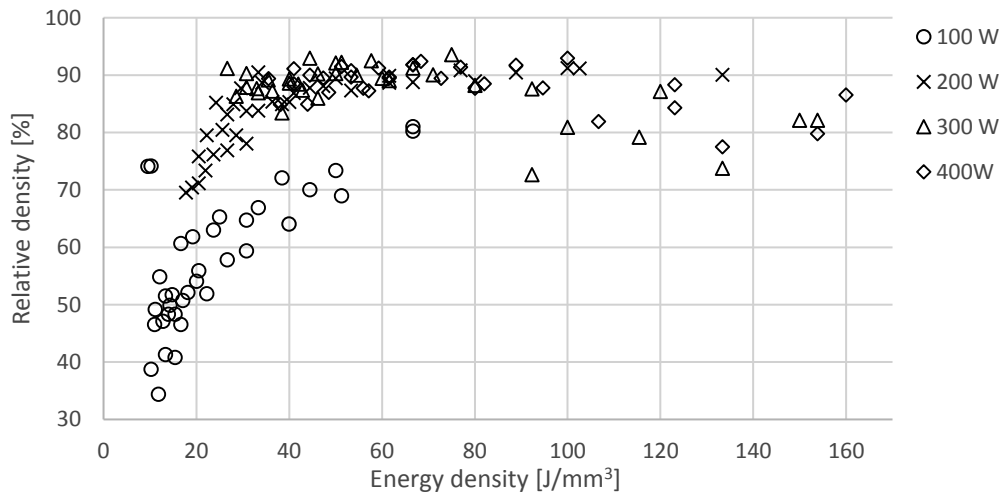


Fig. 6 Influence of energy density on relative density of samples

CONCLUSIONS

In this paper was found that the EN AW 7075 alloy is very difficult to process using SLM technology. Cracks were detected throughout the entire range of process parameters. A range of process parameters were found where the samples contained keyhole pores (low energy density) and the range of process parameters where the samples contained large metallurgical pores (too much energy density). Microstructural analysis showed that cracks are oriented in the direction of scanning. For reduction of hot cracking behavior, the lowering scanning speed and thus lowering temperature gradient during solidification seems to be perspective. Because, as the results show that the amount of cracks is slightly lower for the lower scanning speeds.

ACKNOWLEDGMENT

The research leading to these results has received funding from the Ministry of Education, Youth and Sports under the National Sustainability Programme I (Project No. LO1202). The presented work has been also supported by the Project No. FSI-S-14-2332.

REFERENCES

1. Aboulkhair, N., Everitt, N., Ashcroft, I., & Tuck, C. (2014). Reducing porosity in AlSi10Mg parts processed by selective laser melting. *Additive Manufacturing*, 1-4, 77-86. doi:10.1016/j.addma.2014.08.001
2. Hu, B., & Richardson, I. (2006). Mechanism and possible solution for transverse solidification cracking in laser welding of high strength aluminium alloys. *Materials Science and Engineering: A*, vol. 429(1-2), 287-294. doi:10.1016/j.msea.2006.05.040
3. Kaufmann, N., Imran, M., Wischeropp, T., Emmelmann, C., Siddique, S., & Walther, F. (2016). Influence of Process Parameters on the Quality of Aluminium Alloy EN AW 7075 Using Selective Laser Melting (SLM). *Physics Procedia*, 83, 918-926. doi:10.1016/j.phpro.2016.08.096
4. Li, W., Li, S., Liu, J., Zhang, A., Zhou, Y., Wei, Q., . . . Shi, Y. (2016). Effect of heat treatment on AlSi10Mg alloy fabricated by selective laser melting: Microstructure evolution, mechanical properties and fracture mechanism. *Materials Science and Engineering: A*, 663, 116-125. doi:10.1016/j.msea.2016.03.088



5. Michna, Š., & Lukáč, I. (2005). *Encyklopedie hliníku*. Děčín: Alcan Děčín Extrusions.
6. Montero Sistiaga, M., Mertens, R., Vrancken, B., Wang, X., Van Hooreweder, B., Kruth, J.-P., & Van Humbeeck, J. (2016). Changing the alloy composition of Al7075 for better processability by selective laser melting. *Journal of Materials Processing Technology*, 238, 437-445. doi:10.1016/j.jmatprotec.2016.08.003
7. Olakanmi, E., Cochrane, R., & Dalgarno, K. (2015). A review on selective laser sintering/melting (SLS/SLM) of aluminium alloy powders: Processing, microstructure, and properties. doi:10.1016/j.pmatsci.2015.03.002
8. Prashanth, K., Scudino, S., Maity, T., Das, J., & Eckert, J. (2017). Is the energy density a reliable parameter for materials synthesis by selective laser melting? *Materials Research Letters*, 1-5. doi:10.1080/21663831.2017.1299808
9. Reschetnik, W., Brüggemann, J.-P., Aydinöz, M., Grydin, O., Hoyer, K.-P., Kullmer, G., & Richard, H. (2016). Fatigue crack growth behavior and mechanical properties of additively processed EN AW-7075 aluminium alloy. *Procedia Structural Integrity*(2), 3040-3048. doi:10.1016/j.prostr.2016.06.380
10. Siddique, S., Imran, M., Wycisk, E., Emmelmann, C., & Walther, F. (2015). Influence of process-induced microstructure and imperfections on mechanical properties of AlSi12 processed by selective laser melting. *Journal of Materials Processing Technology*(221), 205-213. doi:10.1016/j.jmatprotec.2015.02.023
11. Tang, M., & Pistorius, P. (2017). Oxides, porosity and fatigue performance of AlSi10Mg parts produced by selective laser melting. *Journal of Fatigue*(94), 192-201. doi:10.1016/j.ijfatigue.2016.06.002
12. Thijs, L., Verhaeghe, F., Craeghs, T., Humbeeck, J., & Kruth, J.-P. (2010). A study of the microstructural evolution during selective laser melting of Ti-6Al-4V. *Acta Materialia*, 58(9). doi:10.1016/j.actamat.2010.02.004
13. Vora, P., Mumtaz, K., Todd, I., & Hopkinson, N. (2015). AlSi12 in-situ alloy formation and residual stress reduction using anchorless selective laser melting. *Additive Manufacturing*, 7, 12-19. doi:10.1016/j.addma.2015.06.003
14. Wei, P., Wei, Z., Chen, Z., Du, J., He, Y., Li, J., & Zhou, Y. (2017). The AlSi10Mg samples produced by selective laser melting: single track, densification, microstructure and mechanical behavior. *Applied Surface Science*, vol. 408, 38-50. doi:10.1016/j.apsusc.2017.02.215
15. Zaretsky, E., Stern, A., & Frage, N. (2017). Dynamic response of AlSi10Mg alloy fabricated by selective laser melting. *Materials Science and Engineering A*, 688, 364-370. doi:10.1016/j.msea.2017.02.004

Corresponding author:

doc. Ing. Daniel Koutný, Ph.D., Institute of Machine and Industrial Design, Brno University of Technology, Faculty of Mechanical Engineering, Technická 2896/2, Brno 616 69, Czech Republic, phone: +420 541 143 356, e-mail: Daniel.Koutny@vut.cz